Suspended Mooring Line Static Analysis using Internal XFlow Capabilities

MIGUEL GIL*, ALEXIA TORRES, JUAN PABLO FUERTES, JAVIER ARMAÑANZAS, JAVIER LEON
Department of Engineering,
Public University of Navarre (UPNA),
Campus de Arrosadia S/N, 31006 Pamplona,
SPAIN

**Corresponding Author*

Abstract: - In the present study, different configurations of a mooring line under a static case are analyzed using the CFD software SIMULIA XFLOW 2022X. Native XFlow geometries employed in the simulation of small springs are used to perform simulations of mooring systems, along with 6 DOF joints, and performing discretization depending on the necessities. Fairlead tensions are compared to experimental data of cables employed in the mooring of DeepCWind semisubmersible platform at 1/40 scale, and to computational model using OPASS. Additionally, the location of different points of the suspended chain in the resting catenary shape is compared to the Quasi-Static model.

Key-Words: - CFD, XFlow, Mooring lines, Static analysis, DeepCWind, FOWT.

Received: March 9, 2023. Revised: December 22, 2023. Accepted: February 24, 2024. Published: April 2, 2024.

1 Introduction

Currently, the use of several CFD software is being employed in the simulation of the dynamics of mooring lines and the integration of simulations with floating platforms for Floating Offshore Wind Turbines (FOWT).

The integration of OpenFOAM and MoorDyn as open-source libraries for the calculation of tensions of mooring lines has been coupled to a body motion solver to update the floating body dynamics, [1].

Coupling DualSPHysics with MoorDyn has also been implemented, [2], for the simulation of the movement of floating structures moored to the sea bottom under the action of different incoming regular waves.

Also, an experimental analysis of hanging suspended chains under static cases for two different chain configurations has been carried out, [3]. An OPASS code, [4], coupled to FAST V6.02 was also implemented and validated under the same case scenario.

In the present paper, SIMULIA XFlow 2022x is employed to simulate a mooring system, and the static tensions of the chain in the fairlead are compared to experimental and computational ones, [3].

Besides, the hanging position of the chain in catenary shape under an equilibrium state is compared to a multisegmented Quasi-Static theory MAP++, [5].

These specific mooring line simulation software work in conjunction with hydrodynamic and aerodynamic load calculation software, which allows to simulation the dynamic behavior of floating wind turbines. With this objective, a co-simulation using Simpack and MoorDyn has been performed, which allows the calculation of average aerodynamic and hydrodynamic loads with AeroDyn and HydroDyn respectively, [6].

Also, the so-called qaleFOAM joint model has been developed to allow the calculation of aerodynamic, hydrodynamic, and mooring loads, used in the simulation of FOWTs, [7].

XFlow is initially designed to perform Aero-Hydrodynamic analysis and integrate the capability of wave generation. [8], by introducing a mooring system in the way that it is discussed in this paper, it is possible to perform the analysis of the full dynamic of a floating offshore wind turbine, avoiding the co-simulations with external software and leading to reduced computational cost, which is the main goal to achieve.

Before analyzing the dynamic behavior of the mooring system, it is necessary to check the chain's

behavior in static cases. This study is the one developed in the present article.

2 Model Data

The mooring line model used in this study consists of cable and joint elements, geometries already implemented by XFlow that are commonly used in the simulation of small springs and dampers. This procedure allows for the discretization of the line in different numbers of segments, which is an aspect that has a great impact on the results and the computational stability.

2.1 Cable Geometry

The cables are introduced defining the points of its ends, so it adopts a stretched cylindrical shape. However, this element is automatically discretized by XFlow once the simulation has started, so it acquires a curvature according to the position of its ends and the physical properties in a certain amount of time, [8], in what is called automatic discretization. To fully define this element, the coordinates of the ends, radius, number of azimuthal segments, density, Young's modulus, second moment of inertia, torsional stiffness, and damping must be determined.

The cable-seabed interaction can be modeled using the restitution coefficient (RC), static friction coefficient (SFC), and dynamic friction coefficient (DFC). A design of experiments (DOE) has been carried out to establish these coefficients, and the results are explained in Section 3.

The cable elements do not interact with the fluid elements, so there are no buoyancy, viscous, or inertia forces due to fluid interaction. However, external forces can be introduced in the global coordinates of the system, acting on the center of gravity of the cable.

As far as the static tests are concerned, the fluid velocity is null, so according to Morison`s equation, there are no external drag forces nor inertia due to its interaction with the fluid. The buoyancy force is expressed as a function of the number of segments in the chain, the total length, the cross-sectional area, and the density of the fluid. In addition, the gravitational force is introduced for each segment. The external force applied on each segment is calculated according to **Σφάλμα! Το αρχείο προέλευσης της αναφοράς δεν βρέθηκε.** 1and corresponds to the net buoyancy, [9], which comprises buoyancy and gravitational forces.

$$F_{ext} = -\frac{L}{n} \cdot A_{trans} \cdot (\rho - \rho_w) \cdot g \qquad (1)$$

The experimental tests, [3], utilize cables employed in the arrangement of the DeepCWind floating platform on a 1:40 scale, and their physical properties are defined in Table 1**Σφάλμα! Το αρχείο προέλευσης της αναφοράς δεν βρέθηκε.**. According to these values, Table 2**Σφάλμα! Το αρχείο προέλευσης της αναφοράς δεν βρέθηκε.** summarizes the parameters introduced in XFlow for the correct definition of the segments that conform to the line.

Table 1. Parameters introduced in XFlow

	Parameters	**Units**
Radio (R)	0.0017	m
Number of azimuthal segments	10	-
Density (ρ)	7599.78	kg/m^3
Young Modulus (E)	3.745E10	Pa
Second moment of inertia (J)	6.56E-12	m^4
Torsional rigidity (K_{tor})	0.921	Nm/deg
Damping (c)	245.06	Ns/m
Static friction coefficient	1	-
Dynamic friction coefficient	1	-
Restitution coefficient	0.05	-
External force per segment	[0,-0.334,0]	N

Table 2. Characteristics of the 1:40 scale chain

	Parameters	**Units**
Length (L)	21	m
Mass per unit length (γ)	0.069	kg/m
Line density (ρ_c)	7850	Kg/m^3
Axial stiffness (EA)	3.4E5	N
Equivalent hydro. diameter (D)	0.0034	m

2.2 Joints

The joints allow for the joining of cables and offer 6 degrees of freedom between them. In this way, it allows the discretization of the mooring lines in independent segments. They are massless elements and do not interact with fluid, so they do not alter the behavior of the chain.

2.3 Geometry Setup

Due to the way the mooring lines are constructed in XFlow, and the fact that the initial position of the segments is in cylindrical prism form, the ends of the contiguous segments collide due to the curvature of the cable, as can be seen in **Σφάλμα! Το αρχείο προέλευσης της αναφοράς δεν βρέθηκε.Σφάλμα! Το αρχείο προέλευσης της αναφοράς δεν βρέθηκε.**. Introducing a clearance in between the segments allows for an increase in the stability of the simulations and to reduce internal stresses in the cable.

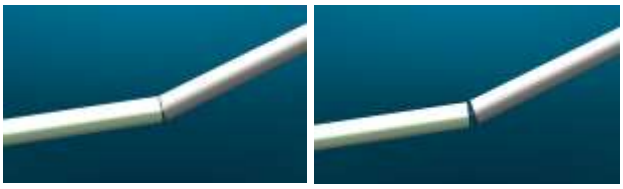

Fig. 1: Internal clearance between segments

As a consequence of the separations of the segments, the transmission of information is reduced and the control over the damping coefficient parameter is lost. This has little effect in static tests but can alter the behavior in the case of dynamic simulations.

2.4 Cable-seabed Interaction

A study of the influence of RC, SFC, and DFC on the cable stress evolution over the simulation time has been carried out. The values shown in Table 1 correspond to the results extracted from this analysis.

The variation of these values does not influence the tension level reached by the chain, nor on the catenary position adopted in a steady state. Therefore, the objective of analyzing these coefficients is to determine the values that allow the results to be obtained in a shorter simulation time. That is to say, to reduce the stabilization time of these simulations.

This effect is observed in Fig. 2, which shows the damping of stresses up to a stationary value, for Cr=0.15, and different values of SFC and DFC.

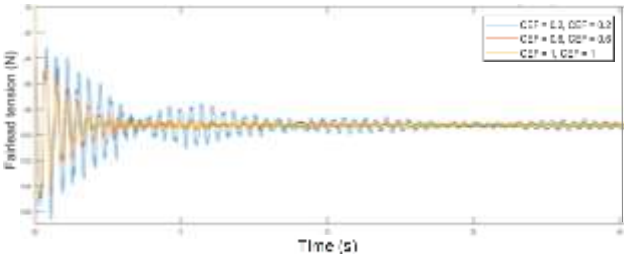

Fig. 2: CR effect on fairlead tension in Configuration 1.

According to the study, CR, SFC, and DFC are set to 0.05, 1, and 1 respectively.

3 Loadcase

To validate the simulation results, the static tests performed in [3], are replicated. These correspond to Case ID 1 and 2, where the difference lies in the position of the fair lead.

The distance between anchor and fairlead X coordinates (d) varies from 19.364 m to 19.872 m depending on the chain configuration, and the fairlead is located 5 m above the anchor, as can be seen in Fig. 3.

Initially, the chain is discretized in 42 segments united by 6 DOF joints, whose initial positions are introduced into the calculation program according to the MSQS model.

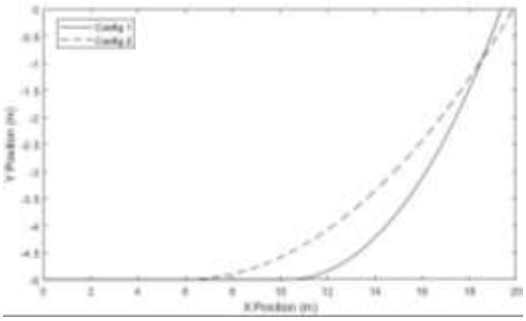

Fig. 3: Simulated models

4 Simulation Setup

Simulations were carried out using SIMULIA XFlow 2022x, a software that employs Lattice Boltzmann technology based on particles for high-fidelity CFD applications. An external, free-surface simulation is performed. Since there is no wire-fluid interaction, 2D simulations are performed, which allows for a decrease in the computational time by reducing the number of elements. Although the domain of the experimental tests is already defined, the domain of the current study is reduced as it does not influence the accuracy of the results, but it does influence the reduction of the simulation cost.

Domain is 30 m long, 1 m wide and 6 m high and a general lattice cell of 0.01 m is established. Inertia forces are also not taken into account, so static equilibrium is reached rapidly from the initial position.

The simulation time is set then to 7 s and 15 s, although equilibrium is reached in 2 or 8 s, depending on the chain configuration.

The total number of elements is 1,800,000, and the simulation time step is set fixed to 0.00111 s. Fig. 4**Σφάλμα! Το αρχείο προέλευσης της αναφοράς δεν βρέθηκε.** shows the simulation setup, displaying in blue each of the joints that connect the segments that make up the chain.

The average simulation time was 3.5 hours with a 12-core, 2.4 GHz processor.

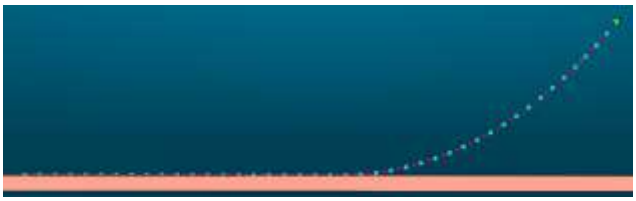

Fig. 4: XFlow Simulation setup

The initial position of the catenary is placed according to Equations (2) and (3), [5]. These expressions also allow us to calculate the tension along the length of the cable, as well as the position along any point of the chain. In these, C_B is the Cable-Seabed friction coefficient, W is the cable weight per unit length, s the cable study point measured from the anchor, EA the axial stiffness, L_B *is* the length of cable in contact with the seabed, H is the horizonal force at the fairlead and L the total cable length.

$$x(s) = \begin{cases} 0 & for\ 0 \le s \le \gamma \\ s + \frac{C_B W}{2EA}[s^2 - 2s\gamma + \gamma\lambda] & for\ \gamma \le sz \le L_B \\ L_B + \frac{H}{W}\sinh^{-1}\left[\frac{W(s-L_B)}{H}\right] + \frac{Hs}{EA} + \frac{C_B W}{2EA}[\lambda\gamma - L_B^2] & for\ L_B \le s \le L \end{cases} \quad (2)$$

$$z(s) = \begin{cases} 0 & for\ 0 \le s \le L_B \\ \frac{H}{W}\left[\sqrt{1 + \left(\frac{W(s-L_B)}{H}\right)^2} - 1\right] + \frac{W(s-L_B)^2}{2EA} & for\ L_B \le s \le L \end{cases} \quad (3)$$

5 Results

This section shows the results extracted from the simulations. To validate the static models, the stresses obtained on the cable fairlead and the position of the cable in the equilibrium position are compared.

5.1 Tension

Fig. 5 shows the evolution of the tension in the fairlead along the simulation time, as well as the tension in each of the principal components for each of the study cases. Initially, the mooring line is discretized into 42 segments for the two configurations. However, the chain in Case ID 2 reaches higher tensions as a consequence of a further fairlead distance relative to the anchor.

This causes a higher instability in the simulation, which is represented in the figure by a longer stabilization time and higher noise in the tension signal. The stabilization time in Config 2 is much longer than 7 s, and the oscillation in the signal once the stable period is reached is excessive.

Therefore, it is decided to reduce the number of segments that compose the mooring line to 21, observing a shorter stabilization time and lower amplitude in the signal oscillations.

The tension is averaged once it has been stabilized, and the results are compared concerning the OPASS model and the experimental results [3]. The error in percentage expresses the difference between the computational results (OPASS and XFlow) concerning experimental ones.

It is observed in Table 3 that the results obtained in terms of fairlead tension are extremely accurate, especially in the case of Config 1, where the error is even lower than the one obtained by the OPASS model. As for Config 2, the error increases, due to the instability of the simulation.

In any case, the errors for both study cases are lower than 3%, which allows the validation of the mooring line model for static analysis where the X coordinate of the fairlead is between 19.364 m and 19.872 m.

Furthermore, it is expected that for d<19.364 m, the error will be less than 0.15%. For tests where d>19.872 m, the error is expected to increase over 2.13%. However, it is possible to further reduce the segment discretization of the lines to increase the stabilization of the simulation.

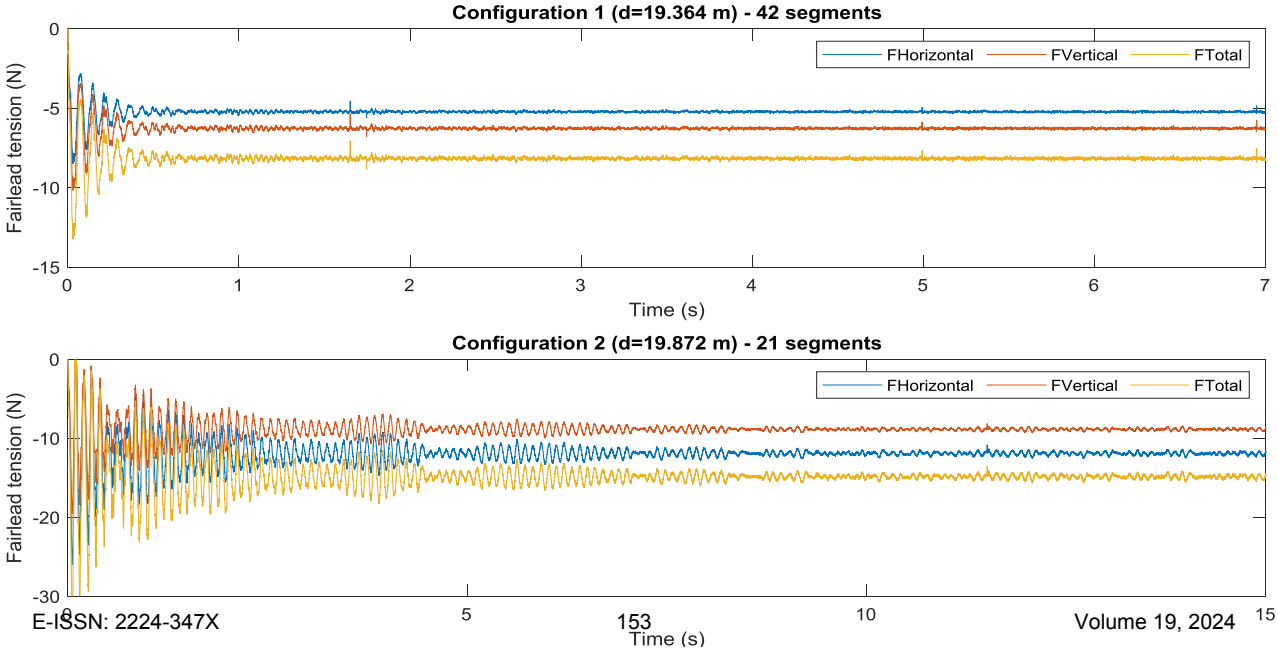

Fig. 5: Fairlead tension evolution along simulation time

Table 3. Fairlead tension in N

	Configuration 1	Configuration 2
Experimental	8.13	14.48
OPASS	8.10	14.70
Difference	0.37%	1.52%
XFLOW	8.14	14.79
Difference	0.15%	2.12%

5.2 Position

It is also important to know the position of the chain once equilibrium is reached.

The catenary shape makes it able to know the chain section that lies on the seabed, which has a great impact on the dynamic interaction of the mooring lines in simulations where the platform is set to freely move.

As above mentioned, the initial position of the segments that make up the mooring line is calculated according to the MSQS model, and it is the theoretical position that should be adopted in a steady state. Therefore, a comparison can be made between the initial and final positions of the joints, and the difference between these positions can be taken as an error in the results.

The positions of the joints have been extracted for both configurations at the final instant of the simulation. Fig. 6 shows the results obtained in XFlow concerning the theoretical values of the MAP++ quasi-static model. Additionally, the results of the computational OPASS model concerning the experimental results are shown.

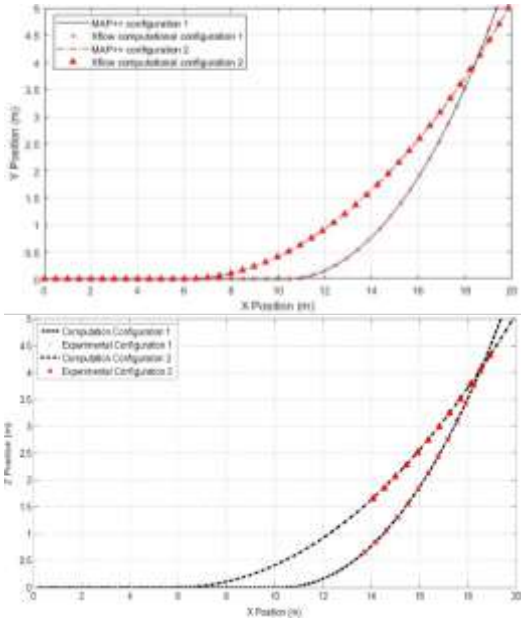

Fig. 6: Catenary coordinates. XFlow (above) and experimental (below)

It shows good agreement between the results obtained in XFlow and the theoretical results. This indicates that, despite the deformation of the segments due to the automatic discretization, there is no elastic or plastic deformation in the material.

To quantitatively check the difference between the initial and final position of the mooring line, and to know the evolution of the simulation, the position of certain points of the chain is shown throughout the simulation time, for both configurations.

Specifically, the evolution of the chain point located at 14 and 18 m from the anchor is monitored, corresponding to joints 29 and 37 in Configuration 1 (Fig. 7), and 15 and 19 in Configuration 2 (Fig. 8), taking into account the different discretization of the cases.

Since the initial position of the joints is very similar to the final one, there is no great evolution in the position over time. The variation in the position of the joints in Config 2 is higher than that observed in Config 1. This is consistent with the error in the static case, which is larger in Configuration 2 than in Configuration 1. Variations close to 10 mm are observed in the vertical coordinate, while the horizontal coordinate is smaller, around 5 mm. However, the fluctuation over time is around the initial point, without observing a positive or negative trend, indicating that the simulation is stable.

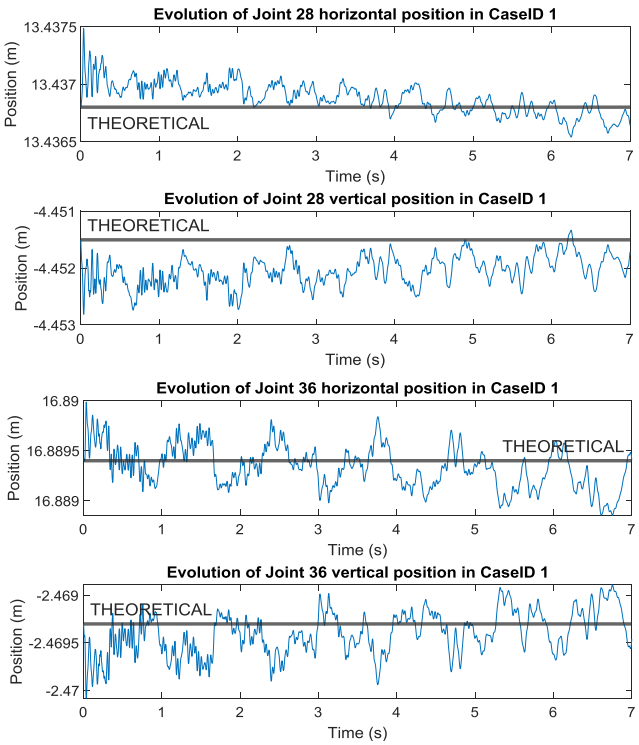

Fig. 7: Evolution in the position of the cable for CaseID 1

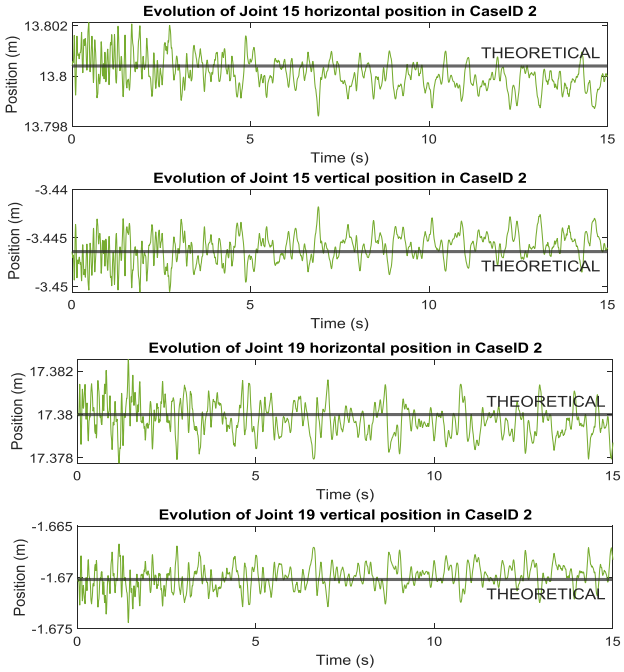

Fig. 8: Evolution in the position of the cables for CaseID 2.

6 Conclusions

In this paper, a new technique has been developed to allow the calculation of static calculation of mooring lines employing SIMULIA XFlow 2022x. Cable and Joint elements have been used, and a manual discretization has been carried out according to the MultiSegmented QuasiStatic model. Two configurations have been studied and the stresses reached in the fairlead and the final catenary shape of the mooring line have been analyzed.

Section 5.1 shows stationary results with reduced error in stresses for both configurations. A reduction of the error in the stationary case below 3% has been achieved, improving the values of the OPASS model for configuration 1. Moreover, according to Section 5.2, it can be confirmed that the cable acquires the catenary shape according to a quasi-static model (MSQS), experimental results, and a computational model (OPASS).

The deviation of the positions concerning the theoretical value calculated by MSQS has been analyzed, observing that these do not differ more than 10 mm in the most unfavorable case (Configuration 2). Therefore, it is guaranteed that the stationary model can correctly represent the behavior of the cables in question. Once the parameters have been established, the cables can be subjected to dynamic and/or semi-dynamic tests.

Acknowledgement:
The authors acknowledge the support from the Government of Navarre (Research project: PC042-043 COSTA).

References:

[1] H. Chen and M. Hall, "CFD simulation of floating body motion with mooring dynamics: Coupling MoorDyn with OpenFOAM," *Applied Ocean Research,* vol. 124, no. 0141-1187, p. 103210, 2022.

[2] J. M. Domínguez, A. J.C. Crespo, M. Hall, C. Altomare, M. Wu, V. Stratigaki, P. Troch, L. Cappietti and M. Gómez-Gesteira, "SPH simulation of floating structures with moorings," *Coastal Engineering,* vol. 153, p. 103560, 2019.

[3] J. Azcona, X. Munduate, L. González and T. A. Nygaard, "Experimental validation of a dynamic mooring lines code with tension and motion measurements of a submerged chain," *Ocean Engineering,* vol. 129, no. 0029-8018, pp. 415-427, 2017.

[4] J. Azcona Armendáriz, X. Munduate Echarri, T. Nygaard and D. Merino Hoyos, "Development of OPASS Code for Dynamic Simulation of Mooring Lines in Contact with Seabed," in *EWEA Offshore 2011 Conference*, Amsterdam, 2011.

[5] M. Masciola, J. Jonkman and A. Robertson, "Implementation of a multisegmented, quasi-static cable model," in *International Ocean and Polar Engineering Conference*, United States, 2013.

[6] M. Y. Mahfouz, T. Roser and P. W. Cheng, "Verification of SIMPACK-MoorDyn coupling using 15 MW IEA-Wind reference models Activefloat and WindCrete," *Journal of Physics: Conference Series,* vol. 2018, p. 012024, 2021.

[7] Z. Yu, Q. Ma, X. Zheng, K. Liao, H. Sun and A. Khayyer, "A hybrid numerical model for simulating aero-elastic-hydro-mooring-wake dynamic response of floating offshore wind turbine.," *Ocean Engineeging,* vol. 268, p. 113050, 2023.

[8] S. Dassault,

XFlow2022x_Golden_UserGuide, Vélizy-Villacoublay, 2022.

[9] M. Hall and A. Goupee, "Validation of a lumped-mass mooring line model with DeepCwind semisubmersible model test data," *Ocean Engineering*, vol. 104, pp. 590-603, 2015.

Contribution of Individual Authors to the Creation of a Scientific Article (Ghostwriting Policy)

The authors equally contributed to the present research, at all stages from the formulation of the problem to the final findings and solution.

Sources of Funding for Research Presented in a Scientific Article or Scientific Article Itself

The authors acknowledge the support given by the Government of Navarre (Research project: PC042-043 COSTA).

Conflict of Interest

The authors have no conflicts of interest to declare.